

TPD and FT-IRAS Investigation of Ethylene Oxide (EtO) Adsorption on a Au(211) Stepped Surface

JooHo Kim[†] and Bruce E. Koel^{*}

Department of Chemistry, University of Southern California,
Los Angeles, California 90089-0482

Received July 30, 2004. In Final Form: February 20, 2005

Adsorption of ethylene oxide, CH₂CH₂O (EtO), on a Au(211) stepped surface was studied by temperature programmed desorption (TPD) and Fourier transform infrared reflection–absorption spectroscopy (FT-IRAS). Ethylene oxide was completely reversibly adsorbed, and desorbed molecularly during TPD following adsorption on Au(211) at 85 K. EtO TPD peaks appeared at 115 K from the multilayer film and 140 and 170 K from the monolayer. Desorption at 140 K was attributed to EtO desorption from terrace sites, and that at 170 K to EtO desorption from step sites. Desorption activation energies and corresponding adsorption energies were estimated to be 8.4 and 10.3 kcal mol⁻¹, respectively. The EtO ring (C₂O) deformation band appeared in IRAS at 865 cm⁻¹ for EtO in multilayer films and when adsorbed in the monolayer at terrace sites. The stronger chemisorption bonding of EtO at Au step sites slightly weakens the bonding within the molecule and causes a small red-shift of this band to 850 cm⁻¹ for adsorption at step sites. EtO presumably binds via the oxygen atom to the surface, and observation of the EtO-ring absorption band in IRAS establishes that the molecular ring plane of EtO adsorbed at step and terrace sites is nearly upright with respect to the crystal surface plane.

Introduction

Ethylene oxide (EtO) is a basic raw material for production of numerous chemical compounds. It is produced industrially via the catalytic epoxidation of ethylene over a promoted Ag catalyst.^{1,2} The high catalytic selectivity (>90%) of this catalyst toward epoxidation (over combustion to CO₂) has drawn much attention. Ethylene epoxidation over Ag catalysts has been extensively studied, and so has ethylene oxide adsorption on Ag single-crystal surfaces.^{3–11} Related surface science experiments have also been conducted on many other metal single-crystal surfaces.

In highly selective catalytic processes, it is important that the desired reaction product does not react further or decompose on the catalyst. Therefore, in discussing catalysts and promoters for ethylene and other olefin epoxidation reactions, it is useful to have basic information about the reactivity of EtO on metal surfaces. Under ultrahigh vacuum (UHV) conditions, it has been reported that EtO is reversibly adsorbed on Ag(110),^{3,4,6,12} Cu(110),^{5–7} Fe(100),⁷ Ni(111),⁷ Ni(110),¹³ Pt(111),¹⁴ and

Pt(110)-(1 × 2).¹⁵ EtO was observed to partially decompose during heating in temperature programmed desorption (TPD) on Mo(111),¹⁶ Rh(111),¹⁷ Pd(111),^{18–20} and in an earlier report on Pt(111).⁹

In this paper, we report on EtO adsorption and desorption on a Au(211) stepped surface at 85 K as probed by primarily TPD and Fourier transform infrared reflection–absorption spectroscopy (FT-IRAS). EtO adsorbed weakly and molecularly on Au(211) with an adsorption energy estimated to be 10.3 kcal/mol at step sites and 8.4 kcal/mol at terrace sites. At either site, IRAS spectra were used to establish an adsorption geometry of EtO such that the molecular plane of EtO is nearly upright with respect to the Au(211) surface.

Experimental Methods

Experiments were conducted in a two-level, stainless steel UHV chamber described previously.²¹ The system had a base pressure of 2 × 10⁻¹⁰ Torr. The lower level was equipped for Auger electron spectroscopy (AES), TPD, and low-energy electron diffraction (LEED) studies, and the upper level had facilities for Ar⁺-ion sputtering and IRAS measurements.

The Au(211) crystal (Metal Crystal & Oxides, Ltd.; diameter 10 mm × 2 mm thick; 5N purity) was mounted using two 0.015-in.-diameter W wires connected to two 0.126-in.-diameter Ta rods pressed into a liquid-nitrogen-cooled Cu block. The crystal could be heated resistively to 1100 K and cooled to 85 K as monitored by a chromel–alumel thermocouple pressed firmly (using Au foil) into a small hole in the side of the crystal. The crystal was cleaned by repeated Ar⁺-ion sputtering (500 eV, 2 μA) for 10 min with the sample at 300 K and annealing at 985

* Corresponding author. Tel: +1-213-740-7036. Fax: +1-213-740-2701. E-mail: koel@usc.edu.

[†] Current address: Battelle-Pacific Northwest National Laboratory, P.O. Box 999/MSIN K8-88, Richland, WA 99352.

(1) Kilty, P. A.; Sachtler, W. M. H. *Catal. Rev.—Sci. Eng.* **1974**, *10*, 1.

(2) Sachtler, W. M. H.; Backx, C.; van Santen, R. A. *Catal. Rev.—Sci. Eng.* **1981**, *23*, 127.

(3) Backx, C.; De Groot, C. P. M.; Biloen, P.; Sachtler, W. M. H. *Surf. Sci.* **1983**, *128*, 81.

(4) Bare, S. R. *J. Vac. Sci. Technol. A* **1992**, *10*, 2336.

(5) Benndorf, C.; Nieber, B. *J. Vac. Sci. Technol. A* **1986**, *4*, 1355.

(6) Benndorf, C.; Krüger, B.; Nieber, B. *Appl. Catal.* **1986**, *25*, 165.

(7) Benndorf, C.; Nieber, B.; Krüger, B. *Surf. Sci.* **1987**, *189/190*, 511.

(8) Krüger, B.; Benndorf, C. *Surf. Sci.* **1986**, *178*, 704.

(9) Campbell, C. T.; Paffett, M. T. *Surf. Sci.* **1986**, *177*, 417.

(10) Grant, R. B.; Lambert, R. M. *J. Catal.* **1985**, *92*, 364.

(11) Grant, R. B.; Lambert, R. M. *J. Catal.* **1985**, *93*, 92.

(12) Nieber, B.; Benndorf, C. *Surf. Sci.* **1991**, *251/252*, 1123.

(13) Hamadeh, H.; Knauff, O.; Pirug, G.; Bonzel, H. P. *Surf. Sci.* **1994**, *311*, 1.

(14) Kim, J.; Zhao, H.; Panja, C.; Olivas, A.; Koel, B. E. *Surf. Sci.* **2004**, *564*, 53.

(15) Weinelt, M.; Zebisch, P.; Steinrück, H.-P. *Chem. Phys.* **1993**, *177*, 321.

(16) Serafin, J. G.; Friend, C. M. *J. Am. Chem. Soc.* **1989**, *111*, 6019.

(17) Brown, N. F.; Barteau, M. A. *Surf. Sci.* **1993**, *298*, 6.

(18) Lambert, R. M.; Ormerod, R. M.; Tysse, W. T. *Langmuir*, **1994**, *10*, 730.

(19) Shekhar, R.; Barteau, M. A. *Surf. Sci.* **1996**, *348*, 55.

(20) Shekhar, R.; Barteau, M. A.; Plank, R. V.; Vohs, J. M. *Surf. Sci.* **1997**, *384*, L815.

(21) Wang, J.; Koel, B. E. *J. Phys. Chem.* **1998**, *102*, 8573.

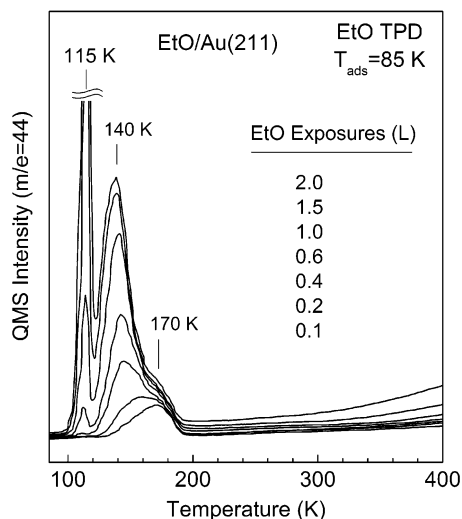


Figure 1. Ethylene oxide (EtO) TPD spectra at $m/e = 44$ for ethylene oxide adsorbed on Au(211) at 85 K. The heating rate was 3 K/s. The EtO TPD spectra are shown directly overlaid, with the results from the lowest exposures causing the smallest peaks near the bottom of the graph and the area under the curves increasing with increasing exposures in the order indicated.

K for 10 min in UHV. This procedure was repeated until the carbon peak in AES ($E_p = 3$ keV) reached a small constant value ($\theta_C \leq 0.02$ monolayer (ML)). After this, the sample at 873 K was exposed to 10^{-5} Torr O_2 for 5 min and flashed to 985 K for 1 min to eliminate any trace of carbon at the surface. After this initial, extensive cleaning procedure, exposure to 10^{-5} Torr O_2 at 873 K for 5 min and flashing to 985 K for 1 min was sufficient to remove any small carbon residue that accumulated at the surface.

Ethylene oxide gas (99.5+% purity; Aldrich Chemical Co.) was dosed on the Au(211) substrate via a stainless steel dosing tube connected to a leak valve. Exposure values are given in units of langmuirs as determined by the background gas pressure in the chamber during dosing with no correction for ion gauge sensitivity. A doser enhancement factor of 5 was utilized in the reported exposures.

TPD experiments were performed with the crystal in line-of-sight of the QMS ionizer and by using a linear heating rate of 3 K s^{-1} . QMS signals at $m/e = 02, 18, 28, 29,$ and 44 were monitored simultaneously. IRAS was obtained by using a Mattson Infinity 60MI spectrometer set at 4-cm^{-1} resolution and accumulating 1000 scans (in 8.5 min).²²

The clean Au(211) surface can be described in microfacet notation as $3(111) \times (100)$, indicating that it consists of 3-atom wide terraces of (111) orientation and a monatomic step with a (100) orientation. A more detailed description, along with a LEED picture from the Au(211) surface, can be found elsewhere.²³

Results and Discussion

TPD Studies. EtO adsorption and desorption on the Au(211) surface was studied by TPD. After exposure of the surface at 85 K to various amounts of EtO, the desorption signals of EtO as well as possible fragments, reaction products, or contaminants were recorded simultaneously.

A series of EtO TPD spectra after increasing EtO exposures is given in Figure 1. EtO desorption was monitored by the signal at $m/e = 44$ which is the parent molecular ion. CO_2 desorption would also produce a signal at $m/e = 44$, but this possibility was eliminated by monitoring the EtO cracking fragment at 29 amu. After small EtO exposures, a single EtO desorption peak was

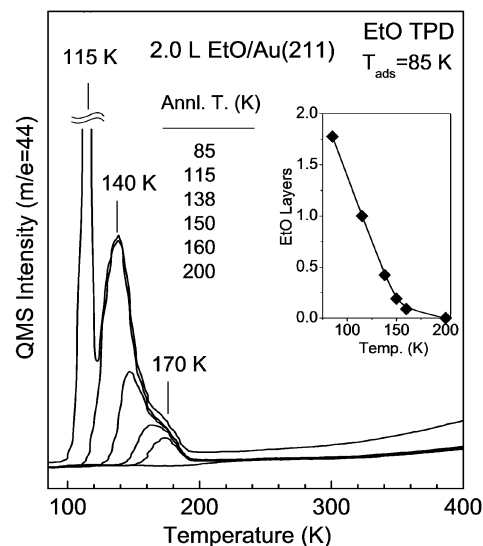


Figure 2. EtO TPD spectra following a 2.0-langmuir EtO exposure on Au(211) at 85 K after heating the surface to 115, 138, 150, 160, and 200 K. The EtO TPD spectra are shown directly overlaid, with the results from the highest annealing temperature causing the smallest peaks near the bottom of the graph and the area under the curves increasing with decreasing annealing temperature in the order indicated. The inset provides a graph of the EtO TPD area and the corresponding adsorbed layer concentration as a function of the annealing temperature. The monolayer coverage was taken to correspond to the area under the EtO TPD peak obtained after annealing to 115 K.

observed at 170 K. With increasing exposures, a second peak started to grow on the low-temperature side of this peak and saturated with the peak at 140 K. Before this peak saturated, a third peak appeared at 112 K. This lowest temperature peak, which shifted to 115 K after higher exposures, arises from EtO desorption from physisorbed or condensed multilayer species. Thus, Figure 1 shows that when EtO was dosed onto the surface at 85 K, desorption occurred from multilayer species even at coverages as low as one-half monolayer. Thus, some condensation into three-dimensional clusters occurs upon exposure at this low temperature prior to filling of the first layer.

The peak at 170 K is from desorption of EtO adsorbed at step sites on the Au(211) surface with a desorption activation energy, E_{des} , of 10.3 kcal/mol, as estimated by Redhead analysis assuming a typical preexponential factor of 10^{13} s^{-1} and first-order desorption kinetics.²⁴ The peak at 140 K is from EtO desorption from terrace sites with a value of $E_{des} = 8.4 \text{ kcal mol}^{-1}$, as estimated in a similar way.

Figure 2 shows TPD spectra after dosing 2.0 langmuir of EtO on Au(211) at 85 K and annealing the surface to 115, 138, 150, 160, and 200 K prior to obtaining the TPD spectra. These data establish that one can form a complete monolayer with no three-dimensional clusters by annealing. Also, such annealing data are necessary to quantitatively measure the amount of EtO in the monolayer at a given temperature. The inset provides a graph of the EtO TPD area and the corresponding adsorbed layer concentration as a function of the annealing temperature. Heating to 115 K removed any condensed multilayer of EtO and left only the monolayer on the surface. The number of EtO layers denoted in the inset was taken to correspond to the area under the EtO TPD peak (one EtO layer) obtained after annealing to 115 K. Heating to 138

(22) Syomin, D. A. Ph.D. Thesis, University of Southern California, Los Angeles, 2001.

(23) Kim, J.; Samano, E.; Koel, B. E. In preparation.

(24) Redhead, P. A. *Vacuum* **1962**, *12*, 203.

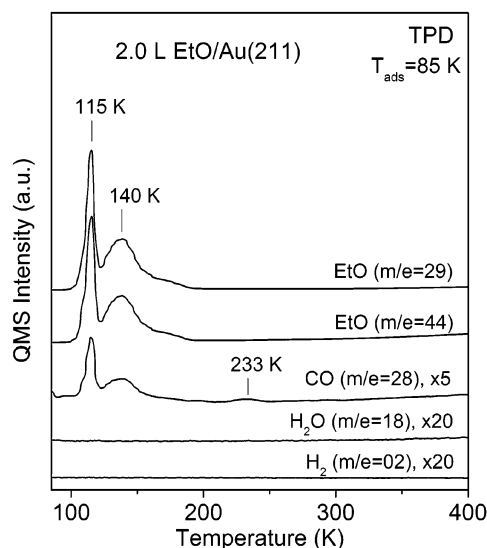


Figure 3. TPD spectra of several gas-phase products after 2.0 langmuir of EtO was exposed on Au(211) at 85 K and flashed to 115 K to remove the EtO multilayer.

K removed some EtO adsorbed on terrace sites, but heating to 150 or 160 K removed all EtO adsorbed on terrace sites, leaving only EtO adsorbed at step sites. The coverage of EtO adsorbed at step sites that one would calculate based on the amount of EtO desorption in the high-temperature state depends on what peak shape one uses for desorption from the step sites. Based on the Au(211) unit cell, one-third of the surface atoms are at steps. If EtO populates step and terrace sites at similar adlayer densities, then the 150 K annealing curve (with an area of 20% of the monolayer coverage) corresponds to desorption from only step sites, but these sites are not yet saturated. If that is the case, the shift to lower temperatures and the change in peak shape arise from repulsive interactions between EtO molecules adsorbed at the step and these interactions appear to be quite strong.

We can make an estimate of the monolayer coverage of EtO on Au(211) referenced to the metal-atom surface density, and this is about 0.25 ML. The basis of this estimate is that we expect nearly close-packing of molecules in the adsorbed monolayer that should be similar on Pt(111) and Au(211) and that the substrate atomic density (1.48×10^{15} atoms cm^{-2}) of Au(211) is similar to that (1.505×10^{15} atoms cm^{-2}) of Pt(111) where the EtO monolayer coverage was proposed to be 0.25 ML.¹⁴

Figure 3 shows TPD spectra at several masses after exposing 2.0 langmuir of EtO on Au(211) at 85 K. The signal at 44 amu is the EtO parent peak, and that at 29 amu is the largest fragment ion of EtO in the QMS. Both of these curves correspond to molecular desorption, and no molecular EtO desorption occurred above 200 K. No desorption of H₂O nor H₂ was detected. The CO TPD spectrum ($m/e = 28$) showed additional peaks that are not fragment peaks from EtO. The peak at 233 K grows with increasing EtO dose on the surface, but we do not believe that either of these CO peaks comes from EtO decomposition on Au(211), but rather from contaminant coadsorption from background gases. CH₄, claimed to be a decomposition product on some metal surfaces,¹⁹ did not appear in our TPD spectra. An uptake curve constructed from the EtO desorption curves (at $m/e = 44$) on Au(211) (not shown here) is a straight line through the origin with increasing EtO dose, which further confirms that there is no decomposition of EtO on the Au(211) surface and 100% of the EtO adsorbs reversibly.

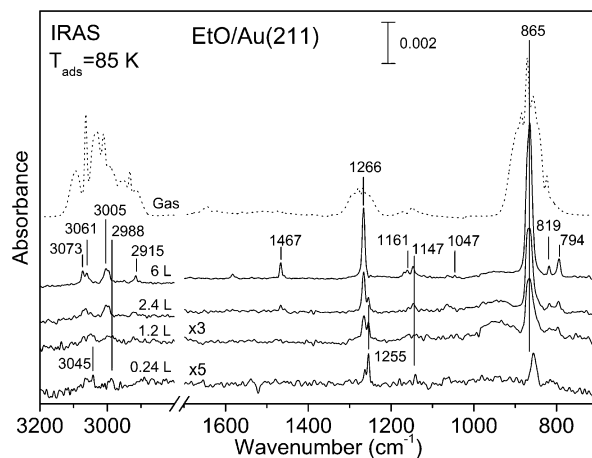


Figure 4. IRAS spectra after increasing EtO exposures (provided for each curve in units of langmuirs (L)) on Au(211) at 85 K. Spectra were accumulated for 1000 scans with a resolution of 4 cm^{-1} . The IR spectrum of gas-phase EtO has been reproduced in the top curve for comparison (adapted from ref 31). The intensities in the two bottom spectra have been scaled by factors of 3 and 5.

These results can be compared to those on a Ag(110) surface, where the EtO TPD peak from the monolayer starts near 165 K at low coverages and shifts about 10 K to lower temperature at saturation monolayer coverage.^{4,8,9} On Cu(110), desorption from the EtO monolayer appears at 190 K and shifts down to 160 K at high coverage.⁷ On Pt(111), EtO desorption from the monolayer shifts from about 200 to 155 K.^{9,14} The EtO desorption peak from the monolayer shifts from 215 to 150 K on Ni(111)²⁵ and from 225 to 170 K on Ni(110).¹⁵ The EtO monolayer peak shifted from 220 to 165 K on Fe(100).⁷ On Ni(110) and Cu(110), another EtO desorption peak at 140 K assigned to desorption from the second layer could be separated from the lower temperature, multilayer desorption peak.^{6,15}

EtO desorption peaks from a saturation coverage in the monolayer on several metal surfaces are quite similar despite the different EtO desorption peaks that are obtained at small coverages. Shifts of the EtO desorption peaks in this regime varied from 10 K on Ag to 65 K on Ni surfaces. This occurs presumably because of the different affinity of the metal substrates toward oxygen atoms. This affinity scales with the metal–oxygen bond strengths, which increase for the series Au, Ag, Pt, Cu, and Ni (e.g., see ref 26). On Au(211), EtO desorption shifted by 30 K as the coverage was increased in the monolayer. This is quite large compared to that on Ag(111) despite a similar affinity of Ag and Au for oxygen. However, this shift arises on Au(211) simply because of the stronger EtO bonding at step sites that are preferentially occupied at low coverages.

FT-IRAS Studies. Figure 4 shows IRAS spectra taken after dosing various amounts of EtO on the Au(211) surface at 85 K. We also provide an IR spectrum of gas-phase EtO as the top, dashed curve for comparison (adapted from ref 31). A 6.0-langmuir EtO exposure deposits enough EtO to form a 5-layer film, and 2.4 langmuir of EtO forms the first and second layers in an EtO film. A dose of 1.2 langmuir of EtO gives a near-saturation coverage in the adsorbed monolayer, and 0.24-langmuir EtO exposure forms about one-fifth of the monolayer coverage.

The most intense EtO absorption band in most of the IR spectra was the ring deformation mode, ν_5 (A_1), at an

(25) Nieber, B.; Benndorf, C. *Surf. Sci.* **1990**, *235*, 129.

(26) Shustorovich, E.; Sellers, H. *Surf. Sci. Rep.* **1998**, *31*, 5.

Table 1. Vibrational Modes of Ethylene Oxide (CH₂CH₂O)

vibrational mode		IR				HREELS					
mode	description	gas (ref 27)	solid (ref 28)	Au(211) [this work]	Ag(111) (ref 29)	Ag(110) (ref 4)	Pd(110) (ref 20)	Pt(111) (ref 9)	Pt(111) (ref 14)	Rh(111) (ref 17)	
ν_1 (A ₁)	CH ₂ stretching	3018	3009, 3004	3005	3000	2960, 3050	2988	2955	3070	3050	
ν_2 (A ₁)	CH ₂ scissoring	1498	1494, 1490			1475	1494	1525	1485	1475	
ν_3 (A ₁)	ring stretching	1270	1263	1266	1267	1250	1268	1380	1270	1240	
ν_4 (A ₁)	CH ₂ wagging	1148	1141, 1133	1147	1148	1145	1147	1110	1160	1140	
ν_5 (A ₁)	ring deform	877	860vvs, 855w	865	869 (860)	847	860	895	866	860	
ν_6 (A ₂)	CH ₂ stretching	3065	3054ms, 3048w				3070				
ν_7 (A ₂)	CH ₂ twisting	1300	1046m, 1040sh	1047							
ν_8 (A ₂)	CH ₂ rocking	860	824w, 818ms	819			770				
ν_9 (B ₁)	CH ₂ stretching	3006	2996ms, 2986s	2998			2988				
ν_{10} (B ₁)	CH ₂ scissoring	1472	1467s, 1460m	1467			1434				
$2\nu_{10}$ (B ₁)	CH ₂ scissoring, overtone		2909mw	2915	2918						
ν_{11} (B ₁)	CH ₂ wagging	1151	1167ms, 1164m	1169			1086				
ν_{12} (B ₁)	ring deform	872	874sh				935				
ν_{13} (B ₂)	CH ₂ stretching	3065	3073w, 3066s	3073, 3061	3070		3070				
ν_{14} (B ₂)	CH ₂ twisting	1142	1158ms, 1152sh	1161			1132				
ν_{15} (B ₂)	CH ₂ rocking	821	794vs, 788vs	794			770				

energy of 865 cm⁻¹ in the multilayer EtO film. At the smallest coverage that we studied, after 0.24-langmuir exposure, this peak shifted 9 cm⁻¹ to 856 cm⁻¹. Stronger bonding at step sites on the surface weakens bonding within the ring and causes the red-shift of the deformation vibrational band. Decreases of 9 and 18 cm⁻¹ were also reported on Ag(111)²⁹ and Pt(111),¹⁴ respectively. We note, in passing, that it may appear that this band shifts higher on Pd(110) after annealing the surface above 280 K.²⁰ However, this “shift” was explained as the appearance of a C–H bending band of methylidyne formed after EtO ring-opening on Pd(110).

IRAS of the thick film after a 6-langmuir EtO exposure shows nearly all of the EtO vibrational modes, even those IR modes that are inactive in the gas phase. Our data are collected in Table 1, along with those for pure EtO in the gaseous and solid phases.^{27,28} Vibrational modes in gas-phase EtO have similar energies as those in the solid phase. Table 1 also shows IR data for EtO multilayer films adsorbed on Ag(111)²⁹ and HREELS data for EtO adsorbed on Ag(110),⁴ Rh(111),¹⁷ Pd(110),²⁰ and Pt(111).^{9,14} Additional discussion of the spectra in Figure 4 will be given below.

Heating the EtO multilayer film can desorb any multilayer species and cleanly prepare monolayer and submonolayer coverages. Figure 5 shows IRAS spectra after 6.0 langmuir of EtO was adsorbed on the Au(211) surface at 85 K and after annealing the surface to 115, 138, 160, and 200 K. The coverages of EtO on the surface after heating, as determined by TPD, were 100, 44, 8.8, and 0% of the monolayer, respectively. Table 2 shows our IRAS data presented in Figure 5 along with IR data from EtO in the solid phase and adsorbed on a Ag(111) surface. Figure 6 illustrates the nature of vibrational modes of EtO in the gas phase, as reconstructed from ref 30.

Other ring-related modes, in addition to the ring deformation mode at 865 cm⁻¹ discussed above, at 1266, 819, and 794 cm⁻¹ are visible in spectra from EtO multilayers and the monolayer. The band at 1266 cm⁻¹ from the ring breathing mode, ν_3 (A₁), splits into two bands at bilayer and monolayer coverages in Figure 4, and this demonstrates two different bonding interactions on the surface. However, IRAS spectra in Figure 5 from annealed

films show only one peak that shifted from 1266 cm⁻¹ in the film at 85 K to 1255 cm⁻¹ in the layer at 160 K. This implies that EtO is present as multilayer and monolayer species after relatively small exposures on the surface at 85 K and rearranges during heating to preferentially occupy only the monolayer. Heating the surface to 160 K selectively populates only step sites, which induces a shift of ring-related vibrational modes to lower wavenumber. This peak shifted by much less, only 4 cm⁻¹, on the Ag-(111) surface during heating from 80 to 140 K.²⁹ So, the presence and influence of step sites are the predominate cause of the 11 cm⁻¹ shift of the ν_3 ring breathing mode and 15 cm⁻¹ shift of the ν_5 ring deformation mode in our IR spectra. Heating to 200 K removes all ethylene oxides from the surface.

We now turn our attention to the C–H stretching vibrational modes that were also observed in our IR spectra of adsorbed EtO. The energies of three C–H stretching bands, due to ν_1 (A₁), ν_9 (B₁), and ν_{13} (B₂) modes, in the multilayer after a 6-langmuir EtO dose on Au(211) at 85 K agree quite well with those from solid-phase EtO.²⁸ In addition to these bands, another feature at 2915 cm⁻¹ was observed. The band at 2915 cm⁻¹ was also seen in the IR data for an EtO multilayer on Ag(111) and in HREELS data for an EtO multilayer on Pt(111) but was not identified.^{29,14} This peak is not likely to be from EtO

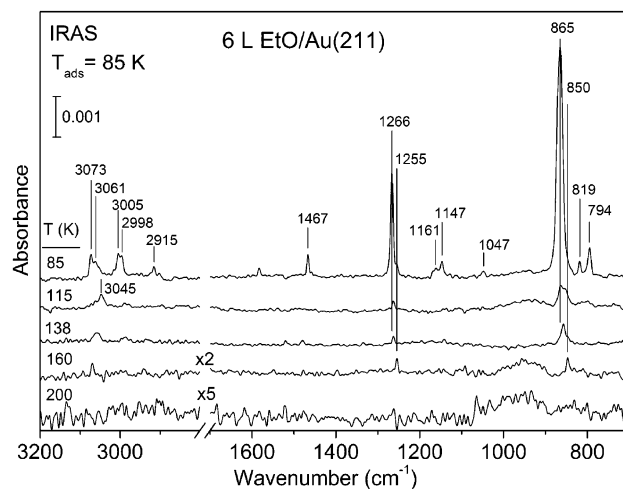


Figure 5. IRAS spectra of a 5-layer film of EtO on Au(211) taken after annealing the surface to 115, 135, 160, and 200 K and cooling to 85 K. Spectra were accumulated for 1000 scans with a resolution of 4 cm⁻¹. The intensities in the two bottom spectra have been scaled by factors of 2 and 5.

(27) Spiekermann, M.; Bougeard, D.; Schrader, B. *J. Comput. Chem.* **1982**, *3*, 354.

(28) Cataliotti, R.; Paliani, G. *Chem. Phys.* **1982**, *72*, 293.

(29) Stacchiola, D.; Wu, G.; Kaltchev, M.; Tysoe, W. T. *Surf. Sci.* **2001**, *486*, 9.

(30) Potts, W. J. *Spectrochim. Acta* **1965**, *21*, 511.

(31) *NIST Chemistry WebBook*; <http://webbook.nist.gov/chemistry/>.

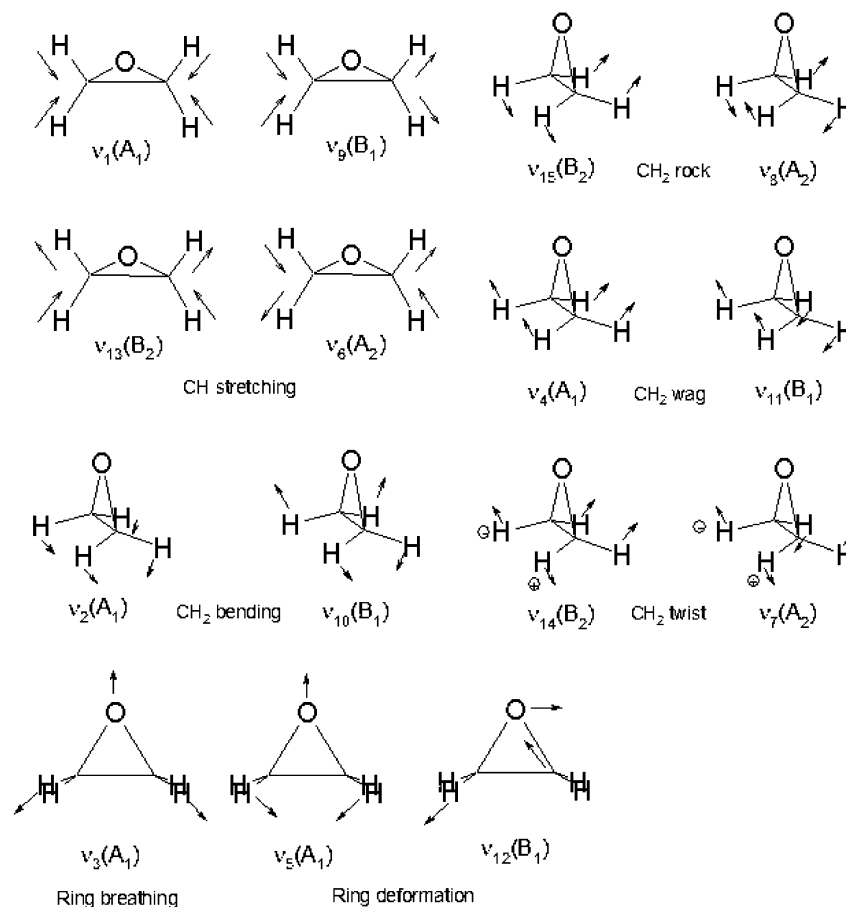
Table 2. Vibrations of Ethylene Oxide Measured by IRAS

vibrational mode		solid phase (ref 28)	Ag(111) (ref 29)		Au(211) [this work]			
mode	description	77 K	80 K (multilayer)	140 K (monolayer)	85 K	115 K	138 K	160 K
ν_{13} (B_2)	CH ₂ stretching	3073w, 3066s	3070		3073, 3061			
ν_6 (A_2)	CH ₂ stretching	3054ms, 3048w				3045	3058	3069
ν_1 (A_1)	CH ₂ stretching	3009, 3004	3000		3005			
ν_9 (B_1)	CH ₂ stretching	2996ms, 2986s	2918		2998			
ν_2 (A_1)	CH ₂ scissoring	1494, 1490				2988	2988	
ν_{10} (B_1)	CH ₂ scissoring	1467s, 1460m			1467			
ν_3 (A_1)	Ring stretching	1263	1267		1266			
ν_{11} (B_1)	CH ₂ wagging	1167ms, 1164m			1169			
ν_{14} (B_2)	CH ₂ twisting	1158ms, 1152sh			1161			
ν_4 (A_1)	CH ₂ wagging	1141, 1133	1148		1147			
ν_7 (A_2)	CH ₂ twisting	1046m, 1040sh			1047			
ν_5 (A_1)	ring deform.	860vvs, 855w	869		865			
ν_{12} (B_1)	ring deform.	874sh			863			
ν_8 (A_2)	CH ₂ rocking	824w, 818ms			857			
ν_{15} (B_2)	CH ₂ rocking	794vs, 788vs	796		850			
					819			
					794			

decomposition, because a similar band was reported in the IR spectrum of solid EtO²⁸ and assigned to an overtone of the CH₂ scissor mode (ν_{10} (B_1)) at 1457 cm⁻¹, as given in Table 1. In the monolayer produced by annealing to 115 K, the most intense absorption band in the CH stretching region appeared at 3045 cm⁻¹. We explain this as arising from the appearance of a new band, not seen in the multilayer spectrum, the ν_6 (A_2) CH stretching mode. Its appearance must arise from a change in the orientation and symmetry of the adsorbate complex in the monolayer. This band shifted to higher wavenumber as the coverage decreased upon annealing to higher temperatures. If bonding to the surface weakens bonding within the ring of EtO, then the CH bonds would be strengthened due to localizing more electrons at the CH bonds and this could explain the blue shift. Such a shift was observed for EtO

adsorbed on Pd(110),²⁰ where a CH stretching band appeared at 3070 cm⁻¹ in the EtO multilayer and shifted to 3080 cm⁻¹ after annealing to 220 K.

We can also obtain information on the orientation of the EtO molecule in the adsorbed monolayer and multilayer films by considering the band intensities and using the metal-surface dipole selection rule. In IRAS, this selection rule means that only bands for totally symmetric vibrational modes with dynamic dipoles (or significant components) that are perpendicular to the metal surface are observed. The band intensities in the gas-phase spectrum given in Figure 4 are indicative of the inherent dynamic dipole moments associated with the vibrations of the molecule. Absorption into a condensed, physisorbed film with a random orientation of the molecules and no strong intermolecular interactions would lead to an IRAS

**Figure 6.** Approximate graphical descriptions of EtO vibrations, as reconstructed from ref 30.

spectrum that closely resembles the gas-phase IR spectrum. However, adsorption is expected to cause additional changes in the IR spectrum because of strong orientation effects within the monolayer, which can be propagated for several layers into the physisorbed film due to electrostatic interactions and packing considerations, and because of bonding interactions (rehybridization and charge transfer) with the Au substrate for molecules within the monolayer.

A comparison of the band intensities in Figure 4 between the spectra for gas-phase EtO and the multilayer EtO film formed by a 6-langmuir exposure shows two noticeable changes in the most intense modes. Relative to the intensity of the ring deformation band at 865 cm^{-1} (ν_5 (A_1)), the intensity of all of the CH stretching modes near 3000 cm^{-1} is decreased and the ring stretching band at 1266 cm^{-1} (ν_3 (A_1)) is increased in the multilayer film compared to that in the gas phase. Furthermore, the relative intensity pattern is not changed dramatically as the coverage is decreased, either by using lower exposures as shown in Figure 4 or by annealing the sample as shown in Figure 5. The schematic drawings in Figure 6 show that all of the CH stretching modes, i.e., ν_1 (A_1), ν_9 (B_1), ν_{13} (B_2), and ν_6 (A_2), have large dynamic dipole components perpendicular to the EtO ring plane, while the ring deformation ν_5 (A_1) and ring breathing or stretching ν_3 (A_1) modes have their dynamic dipole moments parallel to the EtO ring plane. Thus, we conclude that EtO is adsorbed in an upright geometry that has the molecular plane nearly perpendicular to the surface in the monolayer and that this geometry is largely maintained throughout the first several layers of thicker condensed films, presumably via electrostatic or dipolar interactions within the film. Additional small changes in the orientation and symmetry of the adsorbate complex in the monolayer compared to that in the multilayer films are responsible

for the appearance of the CH stretching ν_6 (A_2) band in the monolayer spectra but not in multilayer spectra.

Conclusions

The Au(211) surface can be described by a step-terrace structure consisting of 3-atom wide terraces of (111) orientation and a monatomic step with (100) orientation. These step sites induce about 20% stronger bonding of adsorbed ethylene oxide (EtO) but no additional reactivity under UHV conditions. EtO adsorbed and desorbed molecularly during TPD following dosing on Au(211) at 85 K. EtO TPD peaks appeared at 115 K for the multilayer and 140 and 170 K for monolayer coverages. The peak at 140 K was attributed to EtO adsorbed at terrace sites and the peak at 170 K to EtO adsorbed at step sites on the Au(211) surface. Desorption activation energies were calculated using Redhead analysis as 8.4 kcal mol^{-1} ($T_p = 140\text{ K}$) and $10.3\text{ kcal mol}^{-1}$ ($T_p = 170\text{ K}$), respectively, and these are good estimates of the corresponding adsorption energies.

IRAS spectra showed that the strong band from the C_2O ring deformation mode appeared at 865 cm^{-1} for both EtO multilayer and monolayer films on the Au(211) surface. However, this band shifted to 850 cm^{-1} for EtO adsorbed only at step sites at low coverage. Stronger adsorption bonding of EtO at step sites weakened bonding within the EtO ring and caused a red-shift of the ring deformation mode. The intensity of this and other bands can be used to establish that EtO is adsorbed at both step and terrace sites in an upright geometry with the molecular ring plane nearly perpendicular to the surface.

Acknowledgment. This work was supported by the U.S. Department of Energy, Office of Basic Energy Sciences.

LA0480639